Bar Ilan- Yeshiva University

Summer Science Research Internship Program

INTRODUCTION

The Bar Ilan University-Yeshiva University Summer Science Research Internship Program is an amazing research opportunity for undergraduate men and women, allowing them to contribute to the forefront of science research taking place in Israel. Generously supported by former chairman of Bar Ilan's Global Board of Trustees, Dr. Mordecai D. Katz, and his wife Dr. Monique Katz, and by the J. Samuel Harwit, zt"l & Manya Harwit Aviv Charitable Trust, students gain invaluable laboratory skills, along with an unforgettable summer experience.

Program Director: Professor Ari Zivotofsky
Av and Aim Bayit: Rav Avi and Sara Schwartz

Table of Contents

Editor-in-Chief: Malka Rachel Topp
Editors: Tehilla Berger, Hannah Dubin, & Jacob Stone

Computer Science, Engineering, Math, and Physics

Yael Eisenberg, Rachel Hia, Hannah Dubin, Stephanie Roffe, Benjamin Koslowe, Joseph Rubin, & Aryeh Krischer (not pictured)

Crawling through Google Play

Hannah Dubin
Rachel Hia
Advised under Prof. David Sarne

Before downloading an app or software, many people click "Accept" without reading all, if any, of the Terms and Conditions. Many apps will save user information, such as name, location, gender, and other personal data for different purposes. The user is probably unaware of any unethical clauses in the Terms and Conditions.

Our project aims to create a platform through which consumers can upload a Terms and Conditions document and obtain a short summary of important clauses in the document.

In order to gather a large sample of Terms and Conditions agreements, we wrote a Python program that crawled through the Google Play App Store, using the BeautifulSoup library. A crawler, also called a spider, is a program which can visit many different websites automatically and store the pages for later processing. Once we had the source code for the websites, we used the Python module re to gather the specific attributes of each app, which were inputted into a csv file.

For our platform, the important data from the app is the link to the app's Privacy Policy. Our program wrote the text of these privacy policies

into a text document for each app. We then wrote another script to clean this document. Because every word that appeared on the page for the privacy policy was copied by the program, we had words that were not part of the privacy policy in our document. There are often hyperlinks, such as links to social media sites, often found on the top and bottom of the page, that we did not want to include in our final file. We decided that if we had three consecutive short lines, we could assume that it was not part of the policy, and we should not write it to a cleaner version of the text file.

Once we cleaned the files, by removing leading and trailing short lines, we wanted to use a text processing library to evaluate common themes (patterns, word choice, etc…) included in many of the privacy policies. We would then know exactly which privacy policies contained which themes, and would have to manually assess the accuracy of this division. Once we ensured that each sentence or topic is assigned to the correct general category, we hope that user-inputted Terms and Conditions will be categorized accurately, and our platform will output the specific clauses that are deemed unethical, through supervised machine learning.

Using MEG to Analyze Brain Activity Correlated with Counting and Number Recognition

Yael Eisenberg
Advised under Prof. Mina Teicher and PhD students Ahmad Soleman and Amir Kleks

Magnetoecephalography (MEG, Figure 1) is a non-invasive brain imaging device which detects electromagnetic fields of neurons close to the surface of the head. Because this device uses different techniques than other brain imaging devices, such as functional magnetic resonance imaging (fMRI), it is useful to use the MEG for studying specific sections of the brain, which may be difficult to monitor using other devices. In our lab, we are interested in the identifying where people count in the brain, as a preliminary study. The eventual goal is to figure out the regions in the brain people compute algebra and geometry questions, and observe if those regions differ from one another.

Previous fMRI studies[1] have shown that the IPS (Intraparietal Sulcus, Figure 2) area of the brain is stimulated when people see numbers – whether in digit form (such as: 4) or word form (such as: four). We are trying to take the subject of numerical representation in the brain a step forward. We are researching the location in the brain in which people count small numbers (up to 5). The goal of our experiment is to compare which areas in the brain are stimulated when people count circles vs. sounds vs. taps, and where the brain is stimulated when digits are shown (for the control). Our hypothesis is that the subject's initial reaction to the stimuli will stimulate the area in the brain responsible for visual/audio/sensory, and then the same area in the brain, probably in the IPS will be stimulated. This is because it is clear to the subject that the three as in three circles is identical to three as in three sounds. We will analyze the data we receive from the MEG device using advanced mathematical methods, such as PCA (Principal Component Analysis).

The experiment procedure is as follows: the subject is put in the MEG machine. In part A of the experiment, the subject is shown 2-5 circles (Figure 3), and asked to press a button indicating how many circles he/she sees. There is a 0.7 second break between clicking the amount of circles and the appearance of the next group of circles. For part B, the subject listens to 2-5 beeps, and indicates how many beeps he/she hears. In part C, the subject is

tapped 2-5 times, and indicates the amount of taps. Lastly, in part D, the control part, the subject is shown a digit 2-5, and indicates the digit. Each part of the experiment is repeated 50 times, with part D being repeated just 10 times.

Figure 1. MEG machine

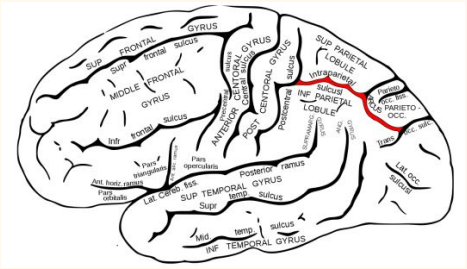

Figure 2. Intraparietal Sulcus (in red)

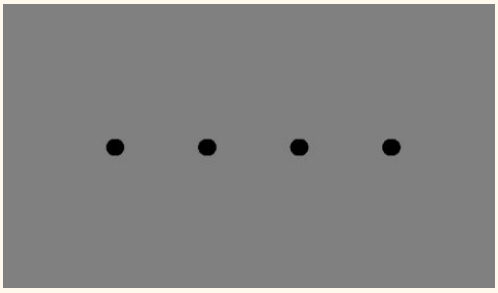

Figure 3. Subject is asked to indicate how many circles appear on the screen.

[1]Probing the Neural Correlates of Number Processing, Andre Knops, 2016

Math Modeling of Natural Killer Cells

Benjamin Koslowe
Advised under Prof. Ramit Mehr and PhD student Lena Fidel

Natural killer cells are lymphocytes, which are part of the innate immune system and are important for early immune responses against viral infections and cancer. Natural killer (NK) cells have two types of receptors – activating and inhibitory. In the last three decades, many receptors, their corresponding ligands, and signaling pathways that regulate NK cell functions have been identified. However, we now know that additional processes, such as NK cell education, differentiation, and the formation of NK cell memory, have a great impact on the reactivity of these cells.

The project to which I contributed dealt with using Mathematical Modeling in order to investigate mechanisms of NK cell signaling. These models involved various hypotheses regarding the nature of the NK cell signaling.

My contribution to the project involved outlining the various hypothesis, as diagrams with corresponding reactions and differential equations. Within the activation model for NK cell signaling, we outlined two models for kinase recruitment and for LCK involvement in the process. Additionally, on the inhibitory side of the picture, we outlined two models for phosphatase recruitment and for LCK involvement in the process. All together this made for 16 different models to predict these processes in NK cells.

The next step in the project will be to test these equations and corresponding parameters with the R computer program. Ideally at least one of the models will successfully establish threshold behavior for NK cells, which means that we

have a good mathematical model for the process.

SQUID – Superconducting Quantum Interference Devices, Investigating and Optimizing Parameters

Aryeh Krischer
Advised under Dr. Beena Kalisky

SQUID, superconducting quantum interference devices, are among the most sensitive magnetic measurement devices ever built and currently the most versatile. At the heart of SQUID physics lies the Josephson Junction, a configuration consisting of a non-superconducting layer sandwiched between two superconductors. In DC SQUID (the type employed here) two Josephson Junctions interrupt an otherwise superconducting loop. These junctions are vital to SQUID operation since, unlike a resistor, when they develop a voltage in the presence of a supercurrent they do not disrupt the flux quantization in the loop. Magnetic flux – field passing through a region of space – through a superconducting loop is quantized which means only whole integer multiples of a fundamental unit of flux (one "flux quantum") can be found in the loop. As a result of this quantization supercurrent in a loop arises to enhance or oppose the ambient field until the flux in the loop reaches the nearest whole number of quanta. SQUIDs are employed for sensitive magnetic measurement by using the voltage developed in the Josephson Junctions to quantify the loop current which in turn is proportional to the magnetic flux through the pickup loop even to small fractions of a flux quantum.

While the above provides a general overview of SQUIDs they are, of course, far more complex in practice, with many different components whose sizes and values can all be tuned. In this project a new batch of SQUIDs with varying parameters were examined in optical, electrical characteristic, and electrical noise surveys. The optical survey was conducted with a simple optical microscope to verify the SQUID components were intact. The electrical characteristic and noise surveys were conducted with two dipping probes for dunking in liquid helium. After the SQUIDs reached approximately 4.2K and became superconducting IV characteristics and measures of bias current to flux quantum conversion were taken. Noise measurements were taken by again cooling the new SQUIDs connected to a special array of SQUIDs designed as an amplifier. This setup allowed the inherent system noise to be observed and measured.

The optical survey revealed that all the SQUIDs were observably intact, and some failed components that had appeared in previous batches were fixed in the present batch. From the electrical characteristic survey resistor values and typical critical current values were found to match fabrication specifications reasonably well. Similarly bias-to-flux ratios were reasonably consistent. Overall only three SQUIDs failed electrically and three others had abnormally large bias-to-flux ratios.

The noise measurements were of particular interest since they sought to determine if the presence of an additional resistor would reduce inherent SQUID noise. First several noise measurements were compared to a SQUID from an older batch. The newer SQUIDs overall had a higher noise floor, but may be tunable to reduce noise. Three pairs of new SQUIDs were also tested to determine the effects of a "damping" resistor. Each pair consisted of two SQUIDs whose physical sizes and resistor values were identical save for a damping resistor on one member of each pair. Both

members of two of the pairs had identical noise floors although the pairs differed from one another. One member of the third pair was abnormally noisy compared to all other SQUIDs measured. From the results of this survey it seems quite clear that the damping resistor has no effect on the noise floor of the SQUIDs.

Using Holographic Maps to interpret FTSTS Maps of Superconductors

Joseph Rubin
Advised under Prof. Emanuele Dalla Torre

Superconductors are of interest because when they are cooled below their critical temperature, they conduct electricity with virtually no resistance. Scientists are searching for new super-conducting materials that have higher critical temperatures, in order to make super-conductivity efficient and economically viable. Understanding the topology of the electron orbitals in the conduction band responsible for super-conductance is the key to knowing which materials to test for super-conductivity.

One tool for studying the conduction band of atoms is Fourier-transformed scanning tunneling spectroscopy (FTSTS). Scanning tunneling microscopes (STMs) create two dimensional subatomic topographical maps of di/dv, the conductance of electrons of atoms in a sample. Each array corresponds to electrons with a constant voltage. Observers cannot discern between the overlapping waves of quasiparticles interfering with each other. Fourier transforming the data, however, isolates the individual wave signals. A Fourier-transform of the 2-dimensional array of the conductance at each point is a 2-dimensional array of complex numbers that represents the sinusoidal signals that make up the original data.

For the super-conductor Bi2201, physicists previously believed that while the magnitudes of the complex numbers of the Fourier transform reveal the periodicity of the Wannier functions of the electrons, the phase is virtually random due to unknown impurities in the sample. Professor Emanuele G. Dalla Torre of Bar Ilan, along with Professor Yang He and Professor Eugene Demler of Harvard, however, showed that by overlapping Fourier amplitudes that differ by reciprocal lattice vectors, the random phase dilations are factored out. They call the resulting map holographic maps, or h-maps, since similar to optical holography, both the magnitude and phase of the data points are relevant. They successfully applied this method to the superconductor Bi2201 and concluded that analyzing holographic maps from STM maps of iron based superconductors may solve “long standing debates about the nature of their conduction bands”[1].

Under the guidance of Professor Dalla Torre, I analyzed iron based superconductors. I applied the method used to analyze Bi2201 to the STM data of FeSe (Iron (II) selenide). My work consisted of three parts: creating a meaningful, visual map of the Fourier transform, creating the h-maps, and making a visual map of the Fourier transform incorporating the new data obtained from the h-maps.

I used Matlab to do a fast Fourier transform of the data. In order to create a visual map of the Fourier transform which contains complex numbers, I displayed the magnitude as the saturation and phase as the hue. Blue corresponds to a phase of 0/360 degrees, red corresponds to a phase of 180 degrees, and shades of purple correspond to phases in-between 0 and 180 and phases in-between 180 and 360. Similar to Bi2201, while the

magnitude was meaningful, the phase appeared completely random (Figure 1).

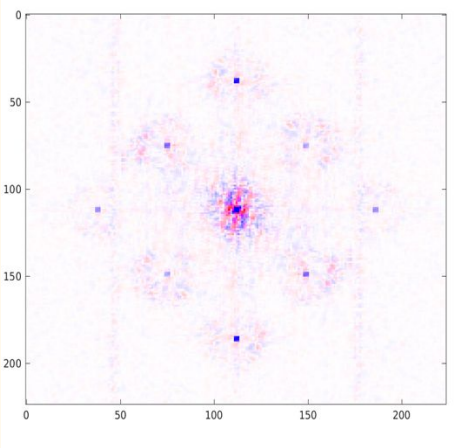

Figure 1. Fourier transform of STM measurements of FeSe.

I then created holographic maps for FeSe. I first analyzed the Fourier transform to find the Bragg's peaks, which are the local maxima in Figure 1 which appear as blue squares. Using Matlab, I first shifted the data in different directions by a lattice vector which reached from one Bragg's peak to the next. For each direction I multiplied the numbers of the original Fourier map by the conjugates of the shifted map. Figure 2 displays the h-maps. The center map is the Fourier transform displayed in Figure 1, and around it are h-maps that correspond to shifts by lattice vectors that point in eight different directions. Unlike the original Fourier transform, the phases in the holographic map have very distinct colors.

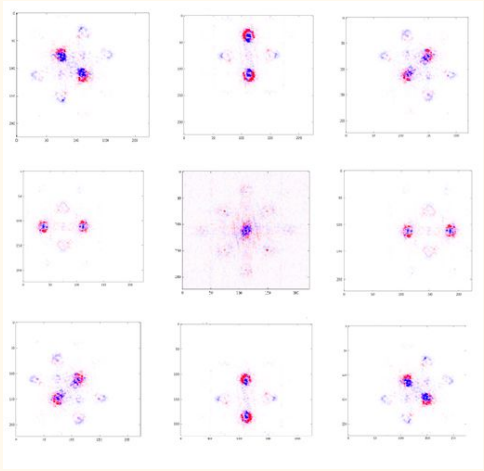

Figure 2. Holographic maps of FeSe.

Based on the holographic maps, we constructed a theoretical map of the Fourier transform with the impurities in the sample factored out (Figure 3).

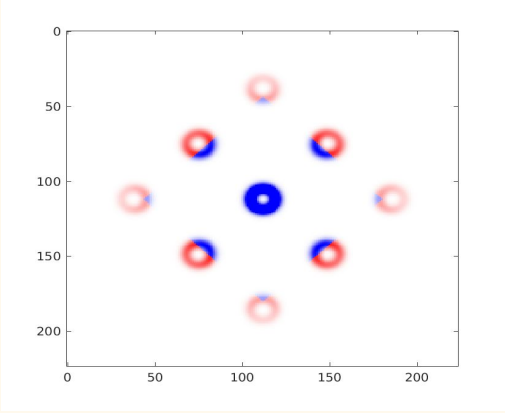

Figure 3. Fourier transform of FeSe with impurities factored out based on h-maps.

In FeSe, the color of the majority of the first Brillouin zone (the four rings closest to the center) is blue, and the second Brillouin zone (the four outer rings) has a tiny bit of blue and the rest is red. The magnitude of the original Fourier transform decreased at the rate of a 2-D Gaussian with a maximum at the center of the map. This theoretical map means that the Fourier transform really corresponds to sinusoidal waves along both diagonals of the

map. The magnitude of these sinusoidal waves is what decreases at the rate of a Gaussian.

Based on the theoretical map, Professor Dalla Torre interprets that each electron in the conduction band of the sample of FeSe is located in a superposition of four Gaussian orbits around four Atoms at the same time arranged as shown in Figure 4. This new information on superconductors brings us closer to finding the next superconductor.

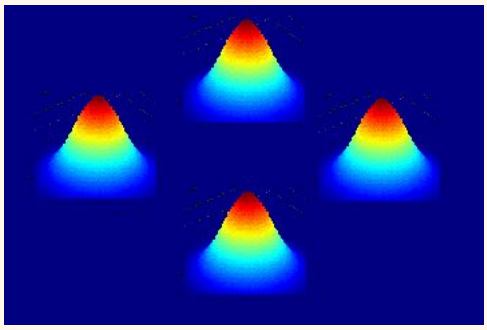

Figure 4. Wave of one FeSe electron, located on a superposition of four atoms.

[1]Dalla Torre, E., He, Y., & Demler E. Holographic maps of quasiparticle interference. *Nature Phys*. **12,** 1052-1056 (2016).

M-280 Dynabeads' Treatment Optimization

Stephanie Roffe
Advised under Dr. Amos Danielli and Dr. Yehudit Michaelson

Background: Fluorescent bio-sensing is a method that was developed in order to detect a target analyte at a low concentration. Detecting molecules at ultra-low concentrations is a challenge, as it faces many limitations, primarily because the laser beam hits only a few molecules. The Magnetic Modulation Biosensor(MMB) system was designed to overcome this challenge, by using magnets to aggregate the fluorescently tagged beads and then measure the signal. This technology is a useful diagnostic tool.

Zika virus comes from the genus Flavivirus. There are many other diseases in this genus such as West Nile, Yellow Fever, and Dengue. It was first identified in Africa during the 1940s, and was named after the forest it was found in, the Zika Forest. Its most recent outbreak was in the Americas, beginning with Brazil in 2015, after which it moved all the way up towards the United States. The Zika virus vector is transmitted through the daytime biting of an urban mosquito known as the Aedesaegypti. Diagnosing Zika is a challenge because its outer proteins are similar to other flaviviruses and are therefore it is difficult to differentiate between them. The most effective way to identify this specific flaviovirus is to to test for the inside NS1 proteins.

To create a rapid NS1 diagnostic test it is necessary to make the technology as effective as possible. By optimizing the binding capacity of the beads, as well as lowering the background noise, the method will have a lower baseline, and thus, an increased sensitivity.

Aim: The aim of this study is to reduce the background noise coming from the beads while maintaining the binding capacity, thereby increasing measurement sensitivity.

Method: This technique is conducted in four stages. In stage one, the beads are treated for 0-hour, 3-hour, 12-hour, and 24-hour. I hypothesized that the longer treatments will experience lower the background fluorescence; however, concurrently, their binding capacity will decrease. In stage two, the samples are split, as I performed an assay. The assay for the M-280 Streptavidin beads is the M-280 dynabead coupled with ATTO 523 Biotin. For the M-280 Tosylactivated beads it is M-280 dynabead coupled to the Zika Virus coupled to human anti NS1 coupled to Anti human 532. After the assay, in stage three, the samples will

be measured by the MMB system. Stage four is the analysis where the data is run through an algorithm.

Results: In experiment 1 the 24-hour treatment is most useful because the signal to noise ratio is 100.0%.

SA Beads	Signal/noise
Non-treated beads	55.6
3h treatment	56.3
12h treatment	68.4
24h treatment	100.0

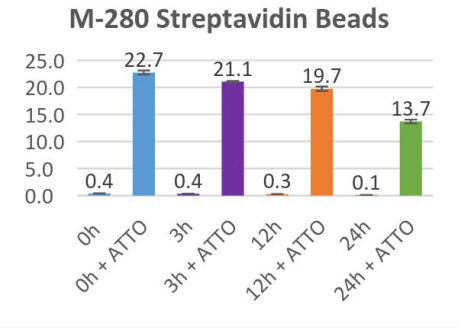

In experiment 2 the 12-hour is most useful because the signal to noise ratio is the highest.

TA Beads	Signal/noise
0hr	14.4
12hr	34.5
24hr	17.3

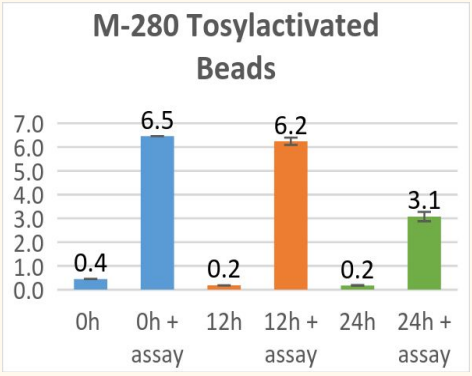

Conclusion: The most effective treatment to reduce background noise is the longest treatment, 24-hours. The M-280 Streptavidin beads had a reduction of 75%, while the M-280 Tosylactivated beads had a reduction of 50%. However, based on the signal/noise ratio, the most effective treatment for the TA is 12-hour, not the 24-hour. The 12-hour treatment has a signal/noise ratio of 34%, in contrast to the 24-hours 17%. However, it only drops the binding capacity by 5%, and the background noise by 50%, while the 24-hour drops it by almost 50%.

Chemistry

Jacob Stone & Tehilla Berger

The Structural Characterization of the CueR Metalloregulator

Tehilla Berger
Advised under Dr. Sharon Ruthstein

Maintaining homeostasis is arguably the most indispensable characteristic requisite to ensure survival and prosperity to all organisms, prokaryotic and eukaryotic alike. Metal ions, in proper levels of concentration, facilitate essential biological processes. Specifically, copper plays a significant and multifaceted role in the human system, such as in its aiding of production of red blood cells, sustaining human systems such as the immune and nervous systems, and perhaps most significantly, regulating DNA transcription. However, in excess, like all metals, its toxicity can prove to be lethal to all organisms. The Ruthstein Lab is thus working on exploring the biological pathways of copper, in hopes to develop a drug that will aide in maintaining copper homeostasis in humans. To do so, it studies the pathways of copper in E. Coli, which was selected as a model because of its presence in the human body.

Under the auspices of Hila Sameach, we are working on examining the function and efficacy of the copper metalloregulator, CueR. Metalloregulators are cytoplasmic or transmembrane proteins, that upon perceiving specific metal substances in high concentrations, induce a reaction. CueR is a

negative repressor, as when it discerns high concentrations of Cu(I), the toxic form of Copper, it induces RNA transcription of two proteins, which aid in regulating copper levels in the cell. The proposed mechanism of CueR's conformation, shockingly, is retained both while bound and unbound to DNA. However, when CueR comes in contact with copper, it undergoes conformational changes, allowing the unraveling of DNA, which in turn allows for RNA polymerase to induce transcription. However, in the absence of copper, the protein conformation does not allow for the unraveling of its DNA, and as such, RNA polymerase cannot bind, and thus, transcription cannot ensue. We studied the CueR protein in various states; isolated, bound to Copper, bound to DNA, and bound to DNA with copper. All states induced a miniscule change in conformation relative to that which we observed in the DNA with copper. Thus, we can ascertain that copper serves as an activator for the CueR metalloregulator by inducing a change in the crystal structure of the CueR metalloregulator.

To better understand this, we utilized the Double Electron Electron Resonance (DEER) technique as a means to study the conformational changes implicit in CueR in the presence of copper. DEER is a form of EPR, which, through isolating the dipolar interaction between two spin probes incited by a set of pulses, we can record data from which we can extrapolate calculations that can measure miniscule distances between 1.5 and 8 nm. The implementation of this technique allows us to explore the structural makeup of the CueR metalloregulator, which is indispensable, as it allows for the survival of E. Coli. This technique is unique and advantageous in that it can study protein samples infinitesimal in size, and provides accurate molecular information regarding the substance, as the substance is tested in solution. However, this method is only capable of depicting a two-dimensional model of the protein.

Using Olivine-Type Materials to Catalyze the Oxygen Evolution Reaction

Jacob Stone
Advised under Prof. David Zitoun and PhD student Yelena Gershinsky

In water electrolysis cells, an electric current is applied to an aqueous solution to split water molecules into hydrogen and oxygen gas. Hydrogen produced by electrolysis cells can then be used as an energy source in fuel cells, where energy is evolved from the combustion of hydrogen gas. Electrolysis cells usually run on solar or wind power, which makes the processes of electrolytic and fuel cells a virtually emission-free source of energy.

The processes of forming oxygen and hydrogen gas from water in an electrolytic cell may be catalyzed using a metal catalyst. Catalysts lower the activation energy for the reaction and thus make the process of electrolysis more efficient. As electrolysis cells become more efficient, fuel cells become a more viable, eco-friendly source of energy.[1]

Part of the Zitoun Lab's research focuses on using olivine-type materials to catalyze the oxygen evolution reaction, which is the half of the electrolysis cell in which oxygen is produced from water. Olivine-type materials such as lithium cobalt (II) phosphate are the materials that make up lithium-ion batteries in mobile phones, and have been well-researched in the field of electrochemistry.[2]

The catalytic activity of olivine-type materials in the oxygen evolution reaction was tested by dropping a liquid suspension that contained some of the material being tested onto an electrode that exhibited limited catalytic activity. After the liquid evaporated, a uniform layer of the olivine-type material covered the catalytically inert substrate. Then, cyclic

voltammetry was used to determine the amount of reaction that occurred in an electrolytic cell across a range of voltages.

It was found that olivine-type materials are efficient catalysts for the oxygen evolution reaction. However, further testing is necessary to determine the stability of these materials in reaction conditions, as it is possible that these materials degrade over time.

---

[1] Vijay Singh, Yelena Gershinsky, Monica Kosa, Mudit Dixit, David Zitoun, Dan Thomas Major (2015). Magnetism in Olivine-type LiCo1-xFexPO4 Cathode Materials: Bridging Theory and Experiment. *Phys. Chem. Chem. Phys.* 2015, 17, 31202.

[2] Masha Alesker, Miles Page, Meital Shviro, Gregory Gershinsky, Yair Paska, Dario Dekel, David Zitoun (2016). Palladium/Nickel Bifunctional Electrocatalyst for Hydrogen Oxidation Reaction in Alkaline Membrane Fuel Cell. *Journal of Power Sources.* 2016, 304, 332-339.

Life Sciences

Top: Miriam Rosen, Malka Rachel Topp, Abby Epstein, Elizabeth Cohen, Lea Lefkowitz, Rebecca Burack, Emily Schwartz, Talia Sanioff, Eitan Lipsky, & Nathaniel Piskin.
Below: Eliana Krim, Adira Teitelbaum, Karen Schaeffer, & Jasmine Naim (not pictured)

Longevity and Proteostasis upon Germline Removal in *C. elegans*

Rebecca Burack
Advised under Prof. Sivan Henis-Korenblit and PhD student Moran Cohen-Berkman

The removal of the germline in *C. elegans* is one method used to slow aging. The hermaphrodite reproductive system of *C. elegans* consists of the somatic gonad, the germ line, and the egg-laying apparatus. Combinations of the gonadal primordium containing Z1-Z4 are removed extending the lifespan of the worm up to 60%. Germline ablation is achieved by mutations in the genes necessary for the proliferation of germ cells. Previous research has shown that the exact transformation from the changes in the reproductive system into the physiological changes, represented as increased lifespan, are unclear.

In this study, endogenous siRNA molecules are found to be associated with the reproductive longevity pathway. It was found that the reduced production of siRNA molecules, shortens the lifespan of those animals. This confirms the importance of siRNAs for the longevity of germless animals. A protein tyrosine-phosphatase (ptp-5) enzyme whose expression is downregulated in germlineless animals and which may be a direct siRNA target, was identified. The reduced expression of ptp-5 restores longevity, improves proteostasis in germlineless animals with defective endogenous siRNA, and increases

survival under heat shock.

Multiple experiments were performed to demonstrate these findings. First, the survival of the strains were tested after heat shock. The strains, in addition to the strains with ptp-5, were placed overnight in heat shock at 37°C for nine hours, followed by a five hour recovery period. We found that siRNA production is critical to resistance to heat shock in long lived animals. Dcr-1 glp-1 has a lower percent survival than that of glp-1. The strains with ptp-5, show an improved survival when comparing dcr-1 glp-1 to glp-1. Additionally, a p value of 0.003 was observed, verifying its significance.

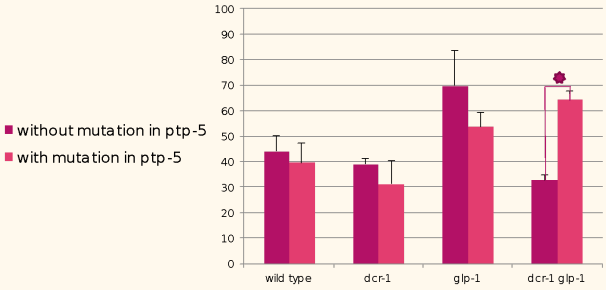

Figure 1. The survival of the strains, in addition to the strains with ptp-5, tested after heat shock.

Second, the number of aggregates formed after heat shock were counted. A ten minute heat shock was applied to the strains at 37°C. Our research had previously shown that introducing ptp-5 to the dcr-1 glp-1 mutation increases the amount of aggregates formed. Furthermore, when comparing wild type and dcr-1 strains with and without the ptp-5 mutation, no significant change was present in the amount of aggregates formed. This new information signifies the specificity of the ptp-5 to the dcr-1 glp-1 mutation.

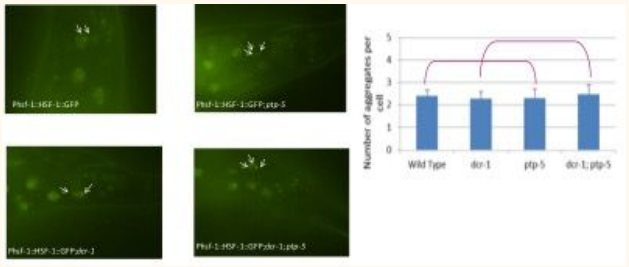

Figure 2. Pictures of the aggregate formation after heat shock in wild type and dcr-1 strains with and without the ptp-5 mutation. No significant change in the amount of aggregates formed was observed.

Third, a proteostasis stress was introduced in this assay. The stress, Q35, causes an accumulation of aggregates in the muscles, similar to Parkinson's Disease. If the worm cannot degrade those aggregates, the animal becomes paralyzed. Q35 was added to day-five glp-1 and dcr-1 glp-1 strains. It was found that the glp-1 mutation, in comparison to the dcr-1 glp-1 mutation, had a greater amount of bends per minute, exhibiting an improvement in paralysis.

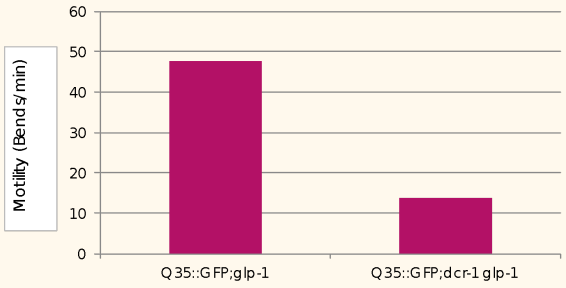

Figure 3. The amount of bends/min observed after the addition of Q35 to glp-1 and dcr-1 glp-1.

Fourth, proteins from *C. elegans* were extracted and exposed to a specific antibody against ubiquitin for the western blot. The thickness of the bends corresponds to the amount of proteins tagged with ubiquitin. A smear on the ubiquitin side was detected corresponding to the many proteins, while one specific bend was

detected on the tubulin side corresponding to the one protein. The tubulin is the control for the amount of proteins loaded and is included in the quantification. Glp-1 mutants have less protein tagged with ubiquitin compared to the wild type. Additionally, the reduced production of siRNA in longevity animals increase the amount of proteins tagged with ubiquitin. We hypothesize that glp-1, in comparison to the wild type, degrades the proteins tagged with ubiquitin, creating a light smear because of a more effective proteasome.

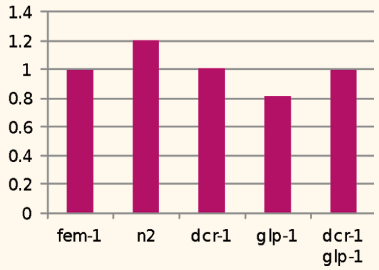

Figure 4. The Western blot and quantifications of the amount of proteins tagged.

Intracellular Dynamics of Beta-Catenin in Response to Wnt Signaling

Elizabeth Cohen
Advised under Prof. Yaron Shav-Tal and PhD student Sarah Hassenson

Beta Catenin, involved in coordination of cell-cell connections, cohesion of centrioles in cell division, and in activating transcription when inside the nucleus, is a protein that when overexpressed, is associated colon cancer, melanomas, medulloblastomas, prostate cancer, and hepatocellular carcinoma. In healthy cells beta catenin binds to a destruction complex in the cytoplasm where it is phosphorylated and then broken down and destroyed. Wnt, a protein that passes signals into cells via cell surface receptors, is involved in the canonical signaling pathway. It inhibits the phosphorylation of beta catenin and allows beta catenin to move into the nucleus and activate genes such as Cyclin D1, which promotes cell division. In cancers ,where the destruction complex is disturbed or mutated and Wnt is not present, inhibition of beta catenin does not take place and it is then overexpressed in the nucleus, promoting excessive cell divisions. Immunofluorescence experiments were conducted in order to show that when Wnt is not present, beta catenin is located only in the cell membrane but not in the nucleus.[1] Fluorescent In Situ Hybridization was also conducted in order to show that when Wnt is present, Cyclin D1 is activated as represented by the fluorescent-tagged transcription site[2]. Western Blot Assay was done with the addition of Wnt in time points of zero to eight hours where two hours contained the greatest concentration of beta catenin.[3] In the future additional analysis of the canonical Wnt signaling pathway must be done in order to further our understanding of the destruction complex and the protein beta catenin.

[1]https://elifesciences.org/content/5/e16748
[2] ibid
[3] ibid

The TEV Protease and its effect on the Slit-Robo Cell Signaling Pathway

Abby Epstein
Advised under Dr. Yarden Opatowsky and Phd student Michael Sporny

The Slit- Robo cell signaling pathway is widely recognized for mediating axon repulsion in the nervous system. Though it is best known for axon guidance, new functions of this pathway are being discovered each day such as angiogenesis, organ development, and the advancement of cancer. The Slit protein is

secreted as a ligand that binds to a Roundabout (Robo) transmembrane receptor. The Slit protein was first identified in Drosophila and was found to contain three genes, *Slit 1-3,* that encode ~200 kDa proteins. Within these proteins, four Leucine Rich Repeat (LRR) domains were discovered that act as the functional region of the Slit proteins. The Robo protein contains an extracellular domain of five immunoglobulin- like (IG) domains. The LRR2 domain of Slits bind to the IG2 domain of Robo.

Dr. Opatowsky's lab is studying Slit and Robo proteins in order to gain a better understanding of their structure and biochemical behavior with the ultimate goal of engineering cures for neurodegenerative diseases. In order to work with insoluble proteins like Robo, it is necessary to attach a protein tag that will increase the solubility of these recombinant proteins. After the target protein, like Robo, becomes soluble the tag is removed because it has completed its function. The TEV Protease, from the Tobacco Etch Virus and derived from E. Coli, is used to cleave fusion proteins from target proteins. TEV is often utilized to conduct the cleavage due to its high sequence specificity.

We purified TEV proteins and made them available for use. Protein purification began with the transformation of TEV using an expression vector carrying amp resistance. LB/amp plates were used to seed the transformed cells. Then cell growth began after preparing two Liters of 2xYT media. A starter culture was then created through inoculating LB/amp with a colony of the previously prepared transformed cells. After growing the starter overnight, it was centrifuged and the supernatant liquid was removed. The leftover pellet was resuspended in a new 2xYT media, and then it was inoculated into 2 Liters of 2xYT/amp/Cam. It was grown for 4 hours at 35°C while shaking, until the OD reached anywhere from 0.5-0.7. The flask was then induced with 1 mM of IPTG which is used to induce expression. The flask was transferred to a 30°C shaker where growth continued for five hours. The cells were then harvested for centrifugation and were placed in the -80°C freezer. Some of these cells were taken from the freezer and used in lysis, the next step in the purification process. Lysis was then conducted in an ice basket. Two Nickel buffers were prepared for the Nickel Column. The 6 histidine tag on the TEV protein it is attracted to the Nickel column, which helps filter out other proteins that do not have a his-tag. Buffer A was used to bind the protein to the column, while Buffer B was used to elute the protein from the column. Three SP-Sepharose buffers were also prepared for the second purification in the column. The SP-Sepharose buffers have a low pH and therefore a positive charge. This attracts TEV, which has a negative charge, and helps filter extraneous parts. Buffer A bound the protein to the column, while Buffer B eluted the protein, and Buffer C diluted the protein. The cells were resuspended until they were thawed and then lysed using a Microfluidizer. TEV was then diluted using SP-Sepharose buffer C and was then loaded onto the column of the AKTA Purifier machine. The flow through was collected. The column was then washed with Nickel Buffer A until no protein was left on the column. Tev was eluted from the column, using Nickel buffer B, and the column was washed again. The protein was run on an SDS Page gel to see if the elution was successful. Then the purification was run a second time using SP Sepharose buffers. Another SDS Page gel was run, to make sure that the second elution was successful and no proteins were left over on the column. Then TEV was concentrated by a Viva Spin column. Glycerol and DDT were added and the protein was put in liquid nitrogen. Then it was stored in -80°C to be used when needed.

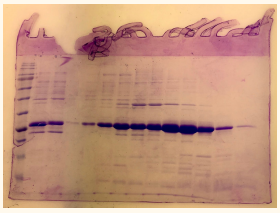
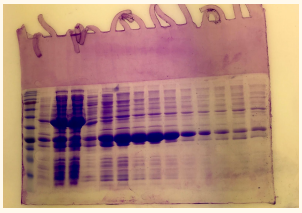

Figure 1 & 2. SDS Page gel after first purification, and SDS Page gel after second purification.

Establishing a New Method of Studying Varicella Zoster Virus (VZV)

Eliana Krim
Karen Schaeffer
Advised under Prof. Ron Goldstein

VZV (Varicella Zoster Virus), or Human Herpes Virus 3 (HHV-3), is a pathogenic human alpha herpesvirus that causes chickenpox (varicella). Initial stages of infection involve inhalation of the virus and an ensuing systemic delivery to the skin, causing itchy, inflamed blisters. Infection also establishes an extended period of latency in the ganglia of the peripheral nervous system (PNS). After a variable interval of time, often decades, the virus usually reactivates, either spontaneously or due to immunosuppression or increased age. The reactivated virus results in shingles (herpes zoster), a disease identified by very painful vesicular skin eruptions, and often accompanied by acute pain, neurological sequelae, vision complications, and enduring post-herpetic neuralgia.

It is difficult to use model systems to study the events related to VZV's latency and reactivation, as the virus is human-specific. Therefore, it is necessary to devise an experimental model for VZV infection and latency. Human neurons, the primary cells involved in VZV are needed to study the virus.

Researchers in Professor Ron Goldstein's lab have created nerve cells using human embryonic stem cells (hESC). However, these hESC-derived neurons are not optimal for use as they are a mixture of both cadaveric sensory neurons (CSN) and peripheral sensory neurons (PSN). The goal of the project is to explore the VZV virus, from the initial hESC differentiation and cell staining, to determining if peripheral sensory neurons – the neurons infected and affected by VZV – can be created using plasmid transfection, through analyzing potential splice sites in its genome.

In the initial stage of the project, an immunofluorescent double- staining protocol was performed in order to observe if the hESC-derived neurons were PSN. Anti-neurofilament was applied to suspected neurons, and a microtubule stain served as the control. This protocol was successful, showing that the hESC-derived neurons differentiated into neurons, as all but one antibody stained in a manner that indicated such.

The Goldstein Lab uses stem cells from a twenty-year old line in order to create neurons. Since stem cell lines are heavily regulated and replicated many times, their quality is often degraded. A study published in 2006[1] demonstrated the ability to push fully-differentiated cells back into pluripotency, thereby increasing researchers' accessibility to stem cells, which they can then differentiate into neurons. The goal of this portion of the project was to determine if human renal cells could be reversed to pluripotency through the use of a bacterial plasmid transfection. *E. Coli* bacteria with plasmids 63726 that code for classic Yamanaka factors (Oct4, Klf4, Sox2, c-Myc and hairpin RNA p53), and bacteria with plasmids 63729 containing Nanog and Lin-28 factors were cultured and transfected with human renal cells. These plasmids also contain fluorescent markers that allow for easy determination of a

successful transfection via fluorescent microscopy. Eventually, these plasmids will be purified from the cells and used to reverse differentiation of cells in order to create pluripotent stem cells. Afterwards, the stem cells will be differentiated into neurons and used in future VZV studies.

Until recently, the model for viral genetics until this point indicated that the viral genome was transcribed and translated directly from the viral genome. However, newer studies[2] suggest that spliced mRNAs play an important role in the action of the virus. Our main project was to test some of the potential splice sites in order to identify true splices and have them sequenced. Eventually, the goal would be to either overexpress or inhibit these spliced mRNAs and see what effect that has on the virus. Two possible splice sites were identified and amplified, using TOPHAT-derived splice sites. In the future, these will be sequenced and either overexpressed or inhibited to determine their roles in the cycle of VZV infection.

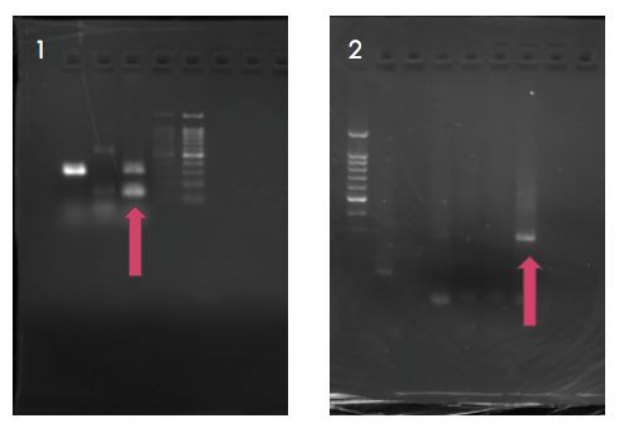

Figure 1 and 2. shows the original gel identifying the splice site. This was purified and PCR was redone on it, resulting in a single band as shown in Image 2.

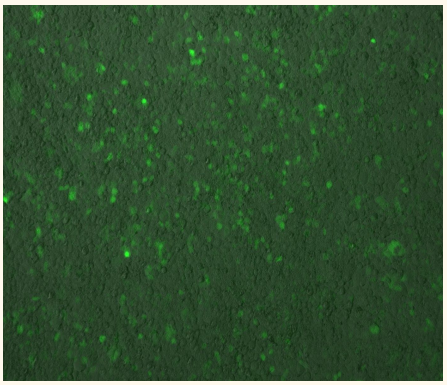

Figure 2. X1000 Control

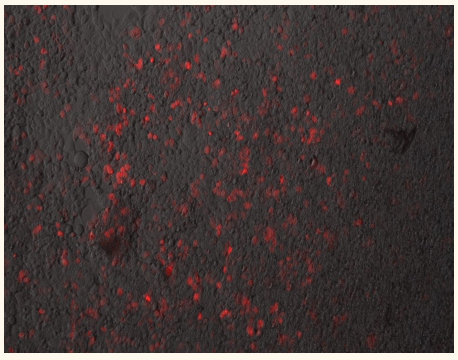

Figure 3. 63729, GFP Transfected (Classic Yamanaka factors)

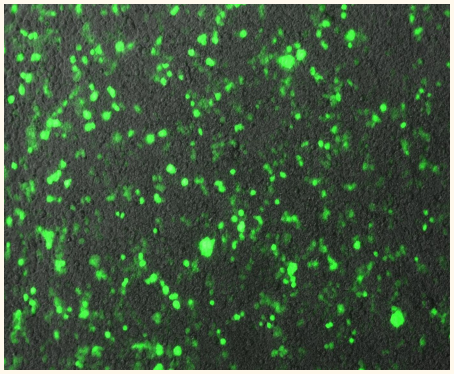

Figure 4. 63726, RFP Transfected

[1]Takahashi, Kazutoshi, and Shinya Yamanaka. "Induction Of Pluripotent Stem Cells From [2]Mouse Embryonic And Adult Fibroblast Cultures By Defined Factors." *Cell*, vol. 126, no. 4, 25 Aug. 2006, pp. 663–676. *Science Direct*, doi:https://doi.org/10.1016/j.cell.2006.07.024.
[3]Zheng, Zhi-Ming. "Split Genes and Their Expression in Kaposi's Sarcoma-Associated Herpesvirus." *Reviews in medical virology* 13.3 (2003): 173–184. *PMC*. Web. 3 Aug. 2017.

Effects of Abiotic Stress on *Arabidopsis thaliana*

Lea Lefkowitz
Advised under Dr. Gad Miller and Dr. Nicholas Rutley

Many plants experience external stress based on their environment and geographical locations. Acute heat and water deficit (dehydration) are two forms of abiotic stress, both of which can have detrimental effects on plant growth. The Miller Lab aims to observe the effects of these conditions, which can be replicated in vitro, on pollen and seed germination. We conducted our research on *Arabidopsis thaliana,* a plant commonly used in scientific research, as well as the first to have its entire genome sequenced. This species is a model organism in that it has certain fundamental qualities which allow experimental results to be quickly and easily obtained. The plant has a short, 8-week life cycle and requires low maintenance. One of the most important qualities of arabidopsis is that phenotypic changes are easily identifiable. The relatively simple nature of arabidopsis enables researchers to expand newly discovered aspects of the plant to more complex plants. Our research consisted of two experiments; the first tested heat stress in pollen, and the second tested both heat and water deficit stress in seedlings. Because arabidopsis can successfully grow between 18°C and 24°C, we exposed the pollen and seedlings to temperatures above this range to observe their effects.

We completed a germination assay on in vitro heat-stressed pollen, which tested mature pollen in the progamic phase. This is the period during which the male pollen grains are transported to the female ovule via the downward growth of the pollen tube. The presence of a pollen tube (PT) confirms successful germination. If a mature pollen grain (MPG) is negatively impacted by acute heat stress, it will not produce a PT. Therefore, the number of PTs relative to the total number of MPGs is inversely proportional to the detrimental effect of that temperature; the more PTs observed at a certain temperature, the weaker the negative effect of heat stress.

The first step is application of short-term heat shock to an aggregate of wild type arabidopsis pollen at different temperatures for 30 minutes. The control group was exposed to a control temperature of 22`C, while the two variable groups were exposed to heat stress at 33`C and 36`C, respectively. We made 3 biological replicates of each group at each temperature. After a 4-hour germination period, we captured 4 images of each replicate via a CellSens live imaging light microscope and counted the number of pollen tubes and total number of mature pollen grains present in each image using ImageJ software. We then used the percentages of PTs and total MPGs in each image to calculate the average percentages at each temperature for further statistical analysis. A decent amount of pollen germination was visible at 22`C, with an average of 11.4% PTs and 88.6% MPGs (Figure 1). At 33`C, there was very little pollen germination, with mean percentages of 7.8% PTs and 92.2% MPGs. Lastly, there was virtually no successful pollen germination at 36`C, with mean percentages of 3.7% PTs and 96.3% MPGs. We found that as temperature rises, the average percentage of PTs decreases due to the pollen's exposure to increased acute heat stress.

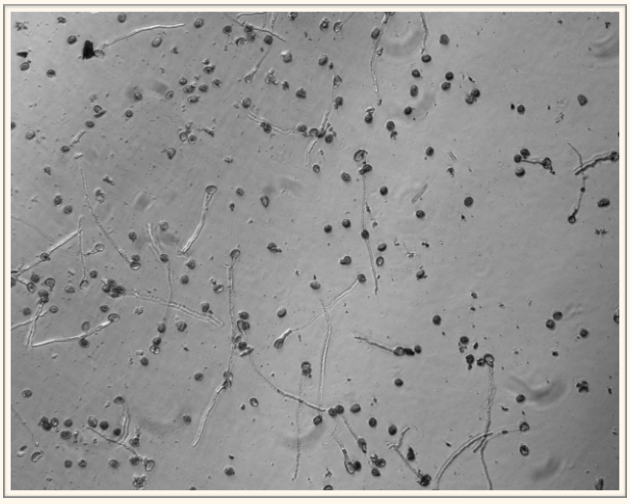

Figure 1. This image was taken using a CellSens live imaging light microscope. It depicts successful pollen germination at 22°C, which is represented by the downward growth of PTs. One MPG is labelled A and one P is labeled B.

Our second study, while following a similar protocol, tracked the effect of heat stress on wild type arabidopsis seedlings, 3 different mutant arabidopsis lines (SALK 089016, SALK 06299, and CS8580783), as well as tested the combined effect of heat stress and water deficit conditions. We induced the additional stress of water deficit by sowing one set of seeds on medium containing 200 uM sorbitol, which causes dehydration. The experiment was two-pronged, and thus required 4 sets of seeds, each with 3 replicates: the first set of seeds was grown on plant-growth medium and was not exposed to heat stress; the second set was grown on medium containing 200 uM sorbitol and was not exposed to heat stress; the third set was grown on plant-growth medium and was exposed to heat stress; and the last set was grown on medium containing 200 uM sorbitol and was exposed to heat stress. On day 5 post-germination, we applied acute heat-stress at 42`C to the experimental groups for 1 hour.

For the week following the heat shock, we observed the phenotypes of the wild type control line and the mutant seed lines in each set, and compared the effects of the heat shock, as well as the effects of the water deficit. Interestingly, we found that the detrimental effect of water deficit was much greater than the effect of the heat shock in all 4 sets. The sets containing 200 uM sorbitol yielded significantly fewer germinated seeds than the control sets at both the control temperature and under heat stress. Heat shock at 42`C does not appear to affect seed growth on control plant-growth medium, except the mutant SALK 089016 seed line, which had limited growth after being exposed to short-term heat shock. Additionally, the mutant SALK 06299 line showed minimal growth under both control and heat stress conditions. Because of the broad relationship between arabidosis and other plants, it is important to continue to study the effects of heat stress and water deficit on arabidopsis. It allows us to gain insight into the mechanisms of agriculture on a larger scale.

Isolating Proteins to Enable Inhibitor Discovery of Sirt6

Eitan Lipsky
Advised under Prof. Haim Cohen and MSc student Matan Avivi

Modern medicine has launched a race to find the key to extending human lifespan. Yet, with all of the developments that have come to the forefront, there has yet to be a solution that allows for extension of life that avoids accompanying metabolic disorder and increase in susceptibility to cancers and other diseases. Professor Haim Cohen's lab studies the mammalian sirtuin proteins, which have a homologue in the Sir2 protein found in yeast, and which have been shown to combine an increase in lifespan with an overall increase in health and reduction of metabolic disorders and diseases. The Sirt6 protein, the main protein studied by the lab, is a NAD+ dependent histone bound deacetylase that

affects metabolic activity. Professor Cohen's lab has shown in the past that the Sirt6 protein has this combination of positive factors. The lab has shown that in mice that have been fed a calorie-restricted diet, which decreases metabolic disorders, there is an increase in expression of Sirt6. Moreover, in mice where Sirt6 was overexpressed while they were fed a typical diet, it was shown that the overexpressed "MOSES" mice showed an increase in health and longevity. The method through which this protein slows aging is not yet entirely clear, but steps are being taken to determine the various molecules that might inhibit Sirt6 in order to be able to develop a drug that would affect its expression in humans and thus be effective in slowing aging.

An important step in the process of inhibiting Sirt6 is determining evolutionarily which amino acid in the protein structure would most likely be the site of a mutation causing changes in its expression. To determine this, we performed an alignment of the amino acid makeup of several of the sirtuin proteins, and identified the points at which the amino acid sequence was conserved. This conservation indicates an early evolutionary history, and thus would be a likely point for a mutation to be able to affect expression. In order to further narrow the search, the distance was measured between each of these conserved amino acids, and the MYK9 substrate that determines much of the protein's activity. After this analysis, it was determined that the most likely location for the mutation would be His133.

To investigate which small molecules influence the expression of Sirt6, the lab will have to perform many activity assays to compare various characteristics of the protein when exposed to the different possible inhibitors. In order to ensure that differences in activity after exposure to an inhibitor are due to the inhibitor's direct influence on Sirt6, and not on a different pathway, the Sirt6 had to be isolated prior to testing. To do so, recombinant Sirt6 was made by inserting it into a PET-28 plasmid. The bacteria was then inspected to see if the Sirt6 was indeed present. To do so, the bacteria was grown in LB growth medium, and added IPTG to induce the protein's expression. After this, the samples were run in a SDS-Page protein gel, and analyzed the results using both Coomasie staining, which binds non-specifically, as well as the specific binding antibodies in Western blotting. Our results showed that Sirt6 was, in fact, present in the bacteria. Future activities of the lab will be to purify the protein contained in this bacteria sample, and then to proceed with various assays that will indicate which molecules successfully inhibits Sirt6. This molecule would thus be used for developing a drug to control Sirt6's effects in humans.

Searching for gRNA Editing in the Nuclear DNA of Trypanosoma Brucei

Jasmine Naim
Advised under Prof. Ron Unger

The guide RNA (gRNA) editing process is the insertion or deletion of U residues in the mitochondrial mRNA transcripts of kinetoplastid Trypanosomes. Before gRNA editing, the mitochondrial DNA is untranslatable and useless to the Trypanosome. Tripanosoma Brucei, also known as the African sleeping sickness, is a parasitic kinetoplastid belonging to the genus Trypanosoma. Guide RNA heavily edits 9 and mildly edits 3 of the 18 mitochondrial proteins, creating an abnormal base pair distribution among the mitochondrial proteins. We wanted to see if U-editing also occurs in the nuclear DNA of T. Brucei by analyzing all sequences that mapped to the T. Brucei genome, as well as 133 genes that code

for proteins relating specifically to mitochondrial functions.

In comparison to the tally of all the static genes in Tripanosoma Brucei, mapped or unmapped, the mapped sequences contain a slightly higher percentage of A's and G's on average while the mitochondrial genes contain a higher percentage of A's and T's. While the complete genome contains a relatively even distribution of nucleic acids (Figure 1), the mapped mitochondrial related sequences are composed of 29.74% A and 27.05% T.

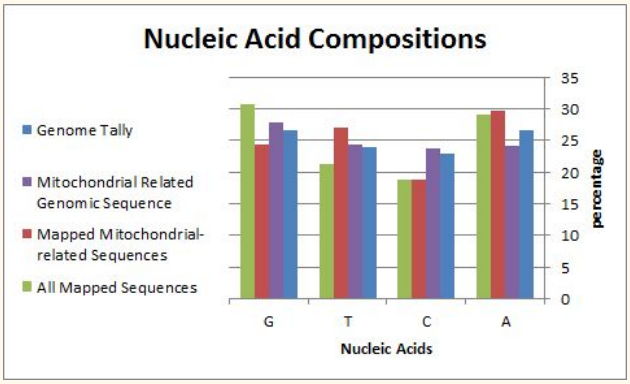

The mapped mitochondrial-related genes are T-rich, but in order to test the validity of this result, we chose 100 samples of 133 random mapped genes and tallied their nucleic acid compositions. After calculating and comparing the RMA values of all sets, we came to the conclusion that the T- rich distribution is not unique to the mitochondrial- related sequences and is just a product of narrowing the set of genes to be tallied.

In order to see if U- editing occurred between the static genome and the mapped sequences, we checked the CIGAR strings of the mapped sequences for an abnormal percentage of insertions and deletions of T's. The percentages of deletions of single nucleic acids in the general mapped tally noticeably differed from the percentages of single nucleic acids deleted in the mitochondrial- related sequences. Much fewer single A's were deleted singularly in the mitochondrial related sequences in comparison to the total mapped sequences. Additionally, more singular T's and G's were deleted in the mitochondrial- related mapped sequences in comparison to all the mapped sequences.

In order to check whether or not this incongruity was significant, we checked one hundred random sets of 133 unique genes and tallied their distribution for single base pair deletions. The RMS values of all the distributions ranged from 1.9 to 52.1 showing that the distributions varied greatly. The RMS of the percentages of single base deletions in the mitochondrial-related sequences lied well within the range of RMS's of the random sets at 35.45, proving that the heavy concentration of single T- deletions is coincidental.

In conclusion, while the distributions of the mitochondrial- related sequences seems unique, there is no proof of U- editing in nuclear DNA that is related to the mitochondria, nor in the nuclear DNA in general.

Regulation of Biofilms in Cyanobacteria

Nathaniel Piskun
Advised under Dr. Rakefet Schwarz and Dr. Eleonora Sendersky

The cyanobacterium *Synechochoccus elongatus* is a common model organism used in laboratory studies of photosynthetic bacteria. Unlike many other cyanobacteria, it forms biofilms, which are microbial assemblages encased in a self-secreted extracellular matrix. Microorganisms in a biofilm display a number of unique morphological and physiological characteristics, among them being a sessile phenotype, lack of piliation, and an altered metabolism. In fact, biofilms often have drastic implications for the fitness of the involved

microorganisms and must therefore be tightly regulated in response to changing environmental conditions.

Biofilms and their regulation in heterotrophic bacteria have been the subject of intense study over the previous decades, especially with regard to their medical applications. However, the molecular mechanisms underpinning biofilm regulation in cyanobacteria have received comparatively little attention. A better understanding of the processes underlying biofilm development could eventually help mitigate the economic loss associated with biofilms, which have been known to cause material decay and blockage through membranes in desalination plants. On the other hand, phototrophic biofilms also have beneficial use cases, such as in wastewater purification systems and in desalination plants. In addition, biofilm based biofuel production systems have been shown to generate high product yields with a minimum input of water and nutrients. When growing cyanobacteria in open ponds, biofilms can also be used as a physical barrier for protection against grazing by small protistan predators, and thus can play an important role in crop protection.

Previous research has shown the negative regulation of biofilm by the T2SE gene, (Type II Secretion System Subunit E) which encodes the ATPase subunit of the Type II Secretion System found in the plasma membrane. Unlike the wild type, the T2SE knockout mutant, or T2SEΩ, displayed a biofilm phenotype, lack of piliation, and decreased protein secretion. In addition, positive regulators of biofilm include the gene cluster EbgG1-4 (Enabling Biofilm Formation through double Glycine motif), and PteB (Peptidase Transporter Essential for Biofilm). The transcript levels of EbfG1-4 and PteB were increased in T2SEΩ, and decreased transiently when T2SEΩ was cultured in wild type conditioned medium. This suggests a model in which T2SE functions in the secretion of a biofilm inhibitory substance into the extracellular space, which then acts on the cell to prevent the transcription of positive biofilm regulators such EbfG1-4 and PteB.

Further candidate genes for biofilm regulation were identified by searching for protein overexpression in T2SEΩ compared to the wild type. Suspected genes were then knocked out on a background of T2SEΩ to see if the biofilm characteristic would be inhibited or attenuated. Knockout was accomplished by transformation of cells with an antibiotic resistance plasmid, and strains were checked for full segregation of chromosomes using PCR and gel electrophoresis. After being grown in liquid culture, strains were quantitatively assessed for the biofilm phenotype using the method of percentage chlorophyll in suspension. The promising candidate genes 1090 and 1370 were identified using these methods, although to confirm their involvement in biofilm regulation, two more biological repeats of the chlorophyll quantification must be performed. Further investigation into these genes will likely confirm their suggested role as positive regulators of biofilms and elucidate their molecular mode of action.

The Role of p53 in Malignant Transformation of MCF10A Cells Mediated by HRAS

Miriam Rosen
Advised under Dr. Ofir Hakim, Dr. Olga Loza and MsC student Bracha Zukerman Attia

In cancer cells, the expression of genes is altered allowing the cells to gain capabilities to promote tumor growth. In regular cells the transcription factor p53 acts as a tumor suppressor, but in over 50% of human cancer cases this transcription factor is mutated.

The transcription factor p53 activates transcription of genes designed to stop cancerous transformation. It activated apoptosis, cell cycle arrest, DNA repair, autophagy, and many other mechanisms involved in preventing carcinogenic transformation.

In previous research, epithelial cells from breast tissue were transformed using the over-expression of HRAS in the MCF10A immortal benign cells to create a cell line used to study the progression of breast cancer. Both the regular MCF10A cells and the HRAS transformed cells were used in this experiment. When the transformed cells were compared with the parental cells the regulatory regions, associated with downregulated genes in the transformed cells, were found to be enriched with a p53 motif. These results were found using RNA-seq, a method used to identify the difference in gene expression between the various cells. It uses next generation sequencing to show the presence and amount of RNA in a biological sample at a given moment.

As shown in the RNA-seq results, there was almost no difference in the expression of p53 between the parental cells and the transformed cells. Therefore, the difference in the genes expression in p53 regulatory areas was not based on the levels of p53 expression, but had to be due to some other mechanism. To figure out the reason for this, the levels of p53 in both types of cell were raised using Nutlin, a competitive inhibitor of MDM2 protein, which is an inhibitor of p53. Nutlin increases p53's transcription, causing it to be more expressed.

Certain genes were chosen for this experiment based on specific criteria. The genes had to be down regulated in the HRAS cancer cells as compared to the MCF10 control cells. They are known p53 targets and have a p53 motif. They have variable chromatin accessibility when compared in the different cell lines. Assay for Transposase Accessible Chromatin with high-throughput sequencing (ATAC Seq) is a method for mapping chromatin accessibility genome-wide, it captures all accessible chromatin sites in the genome. ATAC Seq results show which sites were accessible in the parent cells, but inaccessible in the HRAS cells.

The purpose of this experiment was to validate the results showing changes in gene expression in P53 knock down cells as compared to the normal cells using real- time polymerase chain reaction (PCR). The level of expression of genes in cells of both lines were measured to see the differences between the expression in the cells with Nutlin and those without. Since the threshold of change in these genes' expressions is small, real time PCR was used to record the changes, as it is a sensitive method of measurement, and is able to show the small yet significant differences.

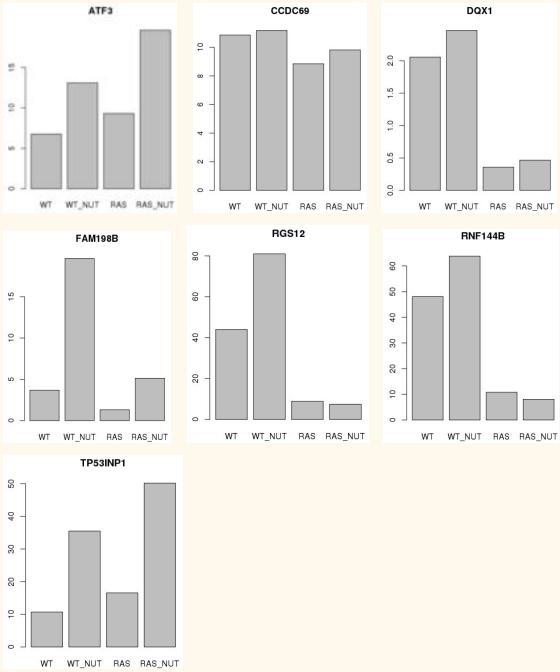

Figure 1. RNA Seq Results for each gene

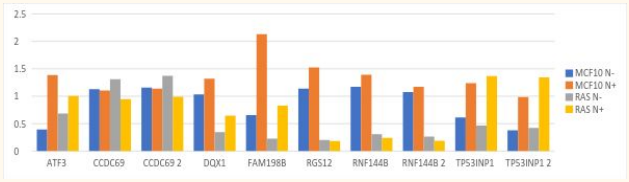

Figure 2. qPCR results for each gene

This experiment tested 7 genes using MCF10A cells and HRAS cells, treating them with Nutlin, extracting their RNA, and normalizing the qPCR results to GAPDH. All of the genes were consistent except for the ATF3 gene and the CCDC69 gene. Most of the genes showed the same changes in expression as the RNA Seq data showed, validating the RNA Seq data. This means that these genes are in fact p53 targets as the RNA Seq data implied and their expression is effected consistently between the regular cells and the Nutlin treated cells.

Antibiotic Resistance in *Pseudomonas Aeruginosa* Examined by the Identification of the Toxin Target Through Gyr A Knockout

Emily Schwartz
Advised under Prof. Udi Banin and PhD student Yitzchak Zander

Pseudomonas aeruginosa is a versatile gram-negative bacterial pathogen that targets a variety of hosts. It is most commonly known for causing chronic infections in patients with cystic fibrosis and is associated with increased morbidity and mortality rates within these patients. Its ability to form a biofilm exacerbates its pathogenic qualities, especially its resistance to antibiotics. A biofilm is a colonization of bacterial cells that attach within an extracellular matrix, secrete an extracellular polymer substance (EPS) and eventually form a protective physical structure. The EPS mainly consists of water, proteins, polysaccharides and nucleic acids that help provide a number of advantages for bacteria such as: protection from harsh environmental conditions, proper nutrition and sustenance, maintaining a consistent population and providing resistance against antimicrobial agents.

Additionally, prophages, also known as viruses, confer various virulent factors by infecting a bacterial host and undergoing the lytic or lysogenic cycle. In the lytic cycle, the virus infects the bacterial host and overpowers the host cell's machinery to produce nucleic acids and proteins required for the production of new virions. This eventually leads to the death and lysis of the cell followed by the dispersal of new virions to infect new host cells and reproduce.

However, in the lysogenic cycle, the bacterial host cell usually remains alive while the virus integrates its DNA within the host cell's DNA and becomes duplicated together during cell division. The viral DNA can either remain in the host cell as a plasmid or can spontaneously switch back to the lytic cycle and lyse the host cell and produce new virions.

Moreover, the prophages that infect the host cells result in different levels of pathogenicity between the varying *P. aeruginosa* strains. This project focused on a toxin-antitoxin system within the PA01 wild type strain of the *P. aeruginosa* to help explain the difference between the variations among the strains. Toxin-antitoxin systems are small genetic modules usually composed of a toxin and an antitoxin counteracting the activity of the toxic protein. For the PA01 strain, a type II toxin-antitoxin system was revealed in which the antitoxins are proteins that sequester, counterbalance toxin activity, or inhibit toxin synthesis. Based on the literature, we proposed the toxin's target is the Gyr A component of the gyrase, which is responsible for uncoiling the tightly wound DNA for replication. Thus, when there is an overexpression of Gyr A, the Gyr A binds to the toxin and prevents the toxin from inhibiting cell growth, and eventually after the cell compensates growth will occur. To test this hypothesis, a growth curve was performed with two different plasmids: PJN, an empty plasmid to serve as the control, and PSSP which is the plasmid containing the toxin. When Gyr A was overexpressed with both of these plasmids there was growth, as expected. However, when the Gyr A box sequence in the gene was deleted, the toxin had no target to bind to, thus allowing toxic activity to occur and preventing cell growth of the host bacteria. This proves that Gyr A is the target site for the toxin that enables the bacterial host cell to continue growing and possess pathogenic qualities.

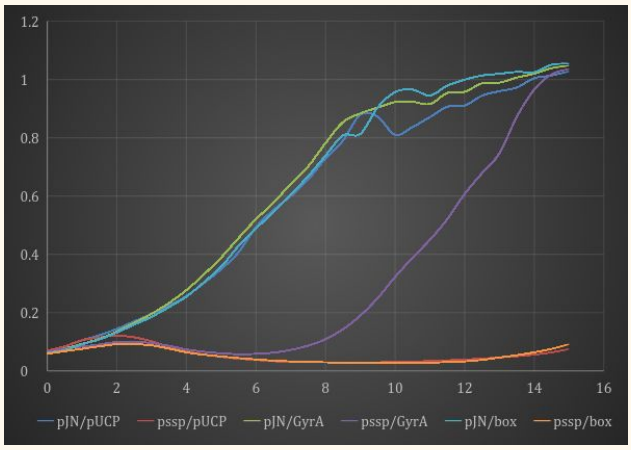

Figure 1. Growth curve results display that without the Gyr A Box sequence to inhibit toxic activity, there was no growth.

Modeling of Rhabdoid Tumor Formation by Pluripotent Stem Cells

Adira Teitelbaum
Advised under Dr. Achia Urbach and PhD student Ilana Gross Carmel

SWI/SNF is a chromatin remodeling complex which is ATP-independent. This complex works to regulate gene expression, and is an active player in epigenetic changes in tumor growth. One of the most fatal pediatric cancers, Rhabdoid Tumors (RT), is formed when there is a loss of functional mutation in the important subunit SNF5. Rhabdoid Tumors are most commonly formed in the brain and kidney. Previous attempts to generate an animal model of RTs of the kidneys have failed. We attempted to create a model through the technique of conditional knock out of SNF5 in multiple lines of human embryonic stem cells. Human pluripotent stem cells (hPSC) are optimal platforms for building disease models due to their pluripotent nature. The SNF5 subunit can be knocked out of the hPSC on the condition of gene overexpression.

In this experiment, we aimed to first generate a line of hPSC (SNF-/-) cells. Once these cells have been successfully generated, we would then generate a new model for RT formation using those hPSC (SNF5-/-) cells. Finally, we would utilize the models generated as a method of studying the molecular mechanism of RT formation. The knowledge gained through these processes can potentially be useful in the development of RT treatment.

In completing step one, the generation of SNF5 conditional function loss in human embryonic stem cells, the cessation of SNF5 had to be prevented through targeting the AAVSI locus with doxycycline (DOX) inducible SNF5, in the HUES13 cell line. This was accomplished through the CRISPR gene editing system, which was then utilized a second time to knock-out the endogenous SNF5. The cells were then electroporated and after 7 days of PURO selection, the colonies were transferred to a new dish to continue growth. Multiple cell lines were tested aside from the HUES13, such as 293T cells and B123 cells, none of which survived except the B123 line, from which one colony was procured. This colony was run on a Polymerase Chain Reaction (PCR) machine, and upon completion, the manipulated DNA was then extracted and tested for insertion. The insertion was successful, but the remainder of the experiment must be completed to finalize the hESC RT model.

Improving Efficacy of Gene Editing with CRISPR

Malka Rachel Topp
Advised under Dr. Ayal Hendel, Dr. Adi Tovin, and MSc student Limor Panet

Background: Gene editing is a powerful new tool for curing genetic diseases. CRISPR, clustered regularly interspaced short palindromic repeats, is a gene editing system made up of a guide RNA and the Cas9 nuclease protein. The guide RNA is about one hundred base pairs long; it is the twenty base pairs at the 5’ end of the guide RNA that directs the cleaving Cas9 protein to a specific location on the genome. The guide RNA hybridizes to a gene by Watson-Crick base pairing near a known point mutation in the gene. The target twenty base pairs can be anywhere on the genome where there is an NGG sequence, the sequence necessary for CRISPR execution, downstream of the CRISPR target site. The Cas9 protein makes a double strand break in the genome three base pairs upstream from the NGG sequence. The cell then repairs the DNA in one of two ways: non homologous end joining (NHEJ) or homologous recombination (HR). In non homologous end joining, the cell repairs the break by inserting and deleting random nucleotides to re-form the gene. This is an effective gene knockout method. Homologous recombination involves the incorporation of new healthy DNA to replace the mutation. This is achieved by administering healthy DNA to the cell simultaneous to insertion of the CRISPR system. It is the CRISPR and HR systems that will together heal genetic mutation.
The CRISPR system is not 100% effective at cutting the gene. Different guide RNAs can achieve different levels of efficacy, which can only be determined experimentally. Severe Combined Immunodeficiency is a genetic disease caused by mutations on the RAG2 gene

on chromosome eleven. Five Guide RNA for the E480X mutation were tested to determine which guide was most effective at cutting out the mutation.

Method: Five guides surrounding the E480X mutation were designed. They were designed as oligos, and annealed using PCR into plasmids containing the genes for the Cas9 protein. These plasmids were inserted into bacteria using Standard heat-shock transformation of chemically competent bacteria. The bacteria were grown for two days and the plasmids procreated inside. The plasmids were then extracted from the bacteria, purified, and sent for sequencing to ensure that they contained the designed twenty base pair guide. When their sequence was confirmed, the plasmids were electroplated into two different cell lines, K562 and Hek293 cells. The cells were grown for three days to allow for CRISPR activity. After that period, the cell's genomic DNA was extracted and then amplified using PCR. The amplified DNA was run on a gel to ensure that the correct gene was amplified. The PCR product is then purified and sequenced using Sanger sequencing. The sequence of the cell that underwent CRISPR was compared to a wild type genome using TIDE Analysis. TIDE analysis measures the frequency of insertions and deletions in the genome.

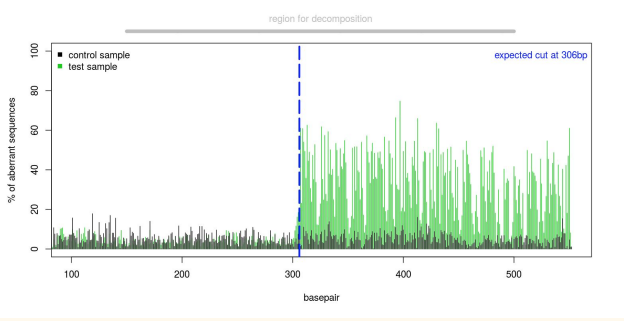

Figure 1. Guide 3 TIDE Analysis. The nucleotide sequence of guide 3 is in green; this is compared to the control sample in black. The blue line indicates the cut site of the CRISPR system. To the left of the line is the area of the gene unaffected by CRISPR; the green and the black are indistinguishable. To the right of the line is the gene after it has been cut with CRISPR. The green is very different from the black, indicating high frequency of insertions and deletions; this illustrates Guide 3's effectiveness.

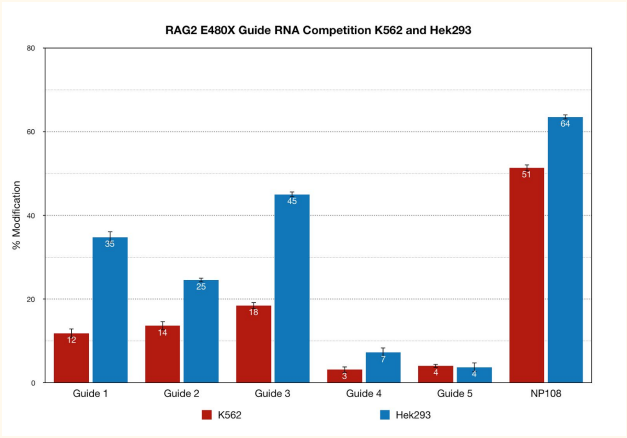

Figure 2. Percent Modification achieved by each of the 5 tested guides plus the NP108 positive control. Guide 3 was the most effective at cutting the genome in both Hek293 and K562 cell lines.

Results: Guide 3 was the most effective at cutting next to the E480X mutation on the RAG2 gene. This is seen in Figure 1 and 2. Guide 3 will be used in future experiments to administer CRISPR along with a healthy gene in order to achieve homologous recombination and ultimately correct the E480X mutation.

Neuroscience

Elisa Alweis, Judy Leserman, Aleeza Dessau, Jennifer Gardner, Zachary Weiss, & Abraham Raichman

Narrative structures of children with and without Specific Language Impairment

Elisa Alweis
Judy Leserman
Advised under Prof. Joel Walters, Prof. Carmit Altman, Prof. Sharon Armon-Lotem, and PhD student Sveta Fichman

Bilingualism is defined as the use of two languages. The study of language development in bilinguals is of unique urgency in Israel because the country is so linguistically diverse. Most Israelis speak Hebrew as their primary language, but other languages, such as English, Arabic, Russian, Yiddish, French, Spanish and Amharic (and 40 other languages) are common. In fact, many citizens grow up speaking two or more languages. Bilinguals experience most of the same language milestones as monolinguals; however, there are certain differences that distinguish them. Research is necessary in order to understand how bilinguals develop language, as well as how to intervene in a classroom setting when there is a discrepancy between the language development of monolinguals and bilinguals.

Specific language impairment (SLI), also referred to as primary language impairment (PLI), affects approximately 7% of school-aged children in the United States (Kohnert, 2010). It is a developmental disorder that can only be diagnosed by ruling out other causes, such as neurological, sensory, cognitive or motor impairments (Ebert, Kohnert, Pham, Rentmeester Disher, & Payesteh, 2014). Though the main feature of SLI is the presence of language delays, there are also deficits in certain cognitive processing skills that have been linked to SLI (Ebert, Rentmeester-Disher & Kohnert, 2012). Bilingual children with SLI

have language delays in both their home language (L1) and their second acquired language (L2). These delays can be difficult to quantify because they must be compared to the language skills of peers who are also bilingual (Ebert et al., 2014). Additionally, even within typically developing bilingual children, their preferred language shifts over time, often moving from greater proficiency in L1 to greater proficiency in L2.

This research focused on studying how bilingualism and SLI relate to one another. The language development of children with SLI presents with the same phenomena that typically developing bilingual children have, such as the omission of verb inflections and prepositions, lexical access, or word-finding problems, etc. This makes diagnosing bilingual children with SLI difficult, as the distinctions between language difficulties that are due to bilingualism, as opposed to those due to a bonafide language impairment are often unclear. However, despite these similarities, bilingualism and SLI require different types of intervention. When the data of typical monolingual development, typical bilingual development, monolingual SLI development, and bilingual SLI are compared, researchers can analyze their differences and similarities, and thus gain insight into how to treat them.

Narratives are an important method for assessment of both SLI and bilingualism because of the wide range of linguistic information stories can provide, such as vocabulary, morpho-syntax, complex syntax, causal relations, and overall story structure. Testing is advantageous, as it takes a relatively short amount of time to conduct. However, analysis of its data is somewhat labor intensive. A significant portion of the speech samples analyzed in this research came from narrative retelling. In this method, a child is told a story and asked by the experimenter to tell the story again. Other samples were elicited by asking a child to tell a story based on a sequence of pictures. Both the retell method and the 'story generation' method allow for comparison between samples.

The data obtained from a narrative can be generally placed into one of two categories, macrostructure or microstructure. Macrostructure refers to the overall structure of a story, and is usually analyzed through story grammar elements. These divide a story into a setting, an initiating event, a goal, an attempt to achieve that goal, and an outcome of the attempt. Each utterance of a narrative can be classified into one of these categories, allowing researchers to see overall trends in the way children structure their stories. For example, Fichman (2017) has found that bilingual children with SLI produce fewer of these story grammar elements and don't have as many connections across episodes in their stories as bilingual children with typical language.

Microstructure, unlike macrostructure, is specific to every language. It includes grammatical aspects such as length, lexis and morphosyntax (Altman et al., 2016). An important microstructural element in bilingual research is code-switching. This occurs when a bilingual speaker applies some aspect of L1 grammar to L2 speech, or vica-versa.

Narrative microstructure was analyzed using the CHILDES and CLAN softwares. Language samples were transcribed and divided into clauses, a unit of grammatical organization that consists of a subject and a predicate. Samples were then coded to indicate errors, error types, mean length of utterance, etc., all of which can be used to assess the progress of a child's language development.

Another possible indicator for differences between bilingualism and SLI relates to fluency, which is analyzed using PRAAT software. This software is used to measure frequency, duration, and other speech fluency

phenomena. As opposed to CLAN, which helps analyze the narrative content and errors in speech, PRAAT measures the length of pauses within and between utterances. Future analyses will look at where pauses occur in an utterance, as well as the macrostructure of the narrative. Though there are no significant results as of yet, the data that has been analyzed as of yet indicates that this information may be useful in identifying characteristics of fluency among bilinguals and children with SLI.

Tourette's Syndrome and Tic Disorder: Understanding the Mechanism to find a Cure

Aleeza Dessau
Advised under Prof. Izhar Bar-Gad and PhD student Esther Vinner.

Tourette's syndrome is a neurodegenerative disease hallmarked by symptoms of tic expression. Tics are defined as sudden, rapid, recurrent, and non-rhythmic movements and sounds. Tourette's syndrome can develop in early childhood and fluctuate with intensity. It can be outgrown by early adulthood. Typically, there are two models used when researching tic expression, the acute model and the chronic model. An acute model is used when investigating short-term phenomena for tics with tic duration lasting approximately one hour. A chronic model is used when studying tic fluctuation over a long period of time, with tic duration lasting for a 7-day period[1].

We used a chronic model in order to study tic expressions and ultimately understand the mechanisms behind tourette's syndrome. A mini-osmotic pump of bicuculline was implanted subcutaneously into the back of a rat (Figure 1). This pump was able to administer fixed doses of bicuculline into the rat's dorsolateral striatum and tics were expressed in the rat's forelimb and head for a 7-day period. Bicuculline is a GABAA antagonist who has the capability to disinhibit parts of the striatum making the rat express unwanted motor movement[2].

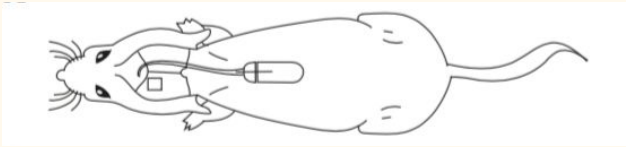

Figure 1. osmotic pump implanted subcutaneously in the back of a rat[3].

Tic expression has been widely correlated to changes in the local field potential (LFP) spikes present in the striatum. Post- operation we conducted several experiments on a chronic model rat and its behavior, and recorded each session. After analyzing the video recordings and the extracellular neural activity, we concluded that tics were expressed during different behavioral states and were highly correlated with the appearance of LFP spikes (Figures 2 and 3).

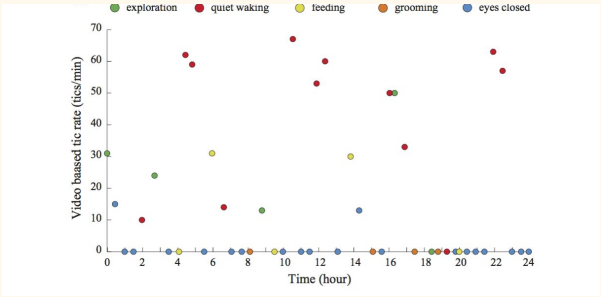

Figure 2. Tics expressed in each behavioral state. Tics were more frequently present per minute in the "quiet waking" state than any other state recorded[4].

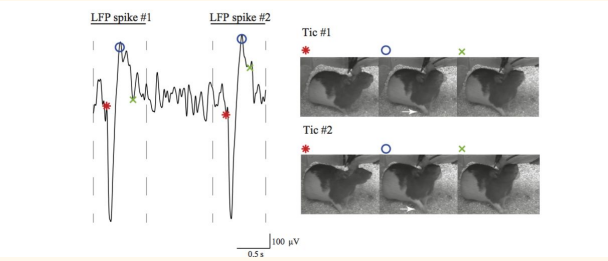

Figure 3. The LFP spikes of neural activity within the striatum are correlated with the outward appearance of tic expression in the rat[5].

The hope is to better understand the mechanism behind Tourette's syndrome and tic expression and can eventually create a sufficient cure to suppress tic expression.

[1] Bronfeld, Israelashvili, Bar-Gad, *Neuroscience & Biobehavioral Reviews*, 2013
[2] Vinner, Israelashvili, Bar-Gad, *JNS methods*, 2017
[3] ibid
[4] ibid
[5] E. Vinner et.al., Prolonged striatal disinhibition as a chronic animal model of tic disorders. J Neurosci Methods, 2017

Molecular Mechanisms of Neurogenesis in the Hippocampal Dentate Gyrus

Jennifer Gardner
Advised under Dr. Eitan Okun, PhD students Sharon Cadury and Yaeli Lev

Neurogenesis is the growth and development of nervous tissue. When one exercises his or her muscles burn because lactic acid is being secreted. There are many articles that state the connection between exercise and neurogenesis. Dr. Eitan Okun's lab found that lactate has an affect on neurogenesis when one exercises. The lactate makes the new neurons survive for longer. They are now testing the behavioral aspect and mechanism of the pathway to see how the lactate affects the neurogenesis.

About a year ago, at the start of this section of research, the lab acquired two groups of mice, one group for the behavioral testing, and one group for the mechanism aspect. Both groups were identical, all male, the same age, and the same species. The group used for the behavioral testing was broken into two groups, each lasting five months. Each of the two groups were broken into five groups, in order to check for five different things: PBS, the control group; Lactate; DHBA, agonist for the GPR81 receptor, the receptor for lactate in the brain; 4CIN, antagonist for MCT-2, the transporter that transports lactate; and 4CIN & Lactate, antagonist to see if the antagonist is working in order to tell if lactate is the mechanism or not.

The behavioral group was injected every day, and then put through a series of tests throughout the five-month period. Some tests were to study long term memory, such as the Barnes Maze, Radial Arm Maze, and Reversal Radial Arm Maze. Other tests were to study short term memory, such as the T Maze and Y Maze. At the end of the five-month period of behavioral tests, they take all of the body parts out of the mouse and freeze it, just in case a body part is needed for the future for further testing.

Figure 1. A slide of the brain slices lined up after the staining.

The mechanism group was given injections every day for six weeks and then their brains were taken out for investigation on September 29, 2016. The brains are prepared as forty micrometer slices, and then an intensive two-day BrdU and NeuN staining is done to them. After picking the first slice containing the dentate gyrus, the part of the hippocampus

that is responsible for memory, every fifth slice is taken in order to get a good sampling. On the first day, the slices are washed five times with phosphate buffered saline with point one percent Triton (PBST), and then the slices sit on the shaker for five minutes between each wash. Then HCl is put into the wells and incubated in 37°C for thirty minutes. HCl is added to increase the surface area, allowing the slices to absorb more antibody. After thirty minutes, Borat Buffer is put into the wells for ten minutes in room temperature in order to neutralize the slices. Next, the slices are washed again with PBST, but this time, two washes are done without shaking in between, and then four more washes with shaking. Next, the blocking, a mixture of twenty percent Normal Horse Serum and eighty percent PBST, is added and set for an hour to shaking. The purpose of the blocking is to make a more specific bonding between the antibody and its target. The last step for day one is to put in the primary antibody, a mixture of 1:1000 anti-BrdU and 1:10,000 NeuN, Neuronal specific marker, diluted in PBST, and two percent Normal Horse Serum. This sits in the slices for three days while shaking in 4°C.

Day two begins with washing the slices five times with PBST and shaking for five minutes each time. Then the second antibody, a mixture of 1:1000 Goat anti-rat 568, and 1:1000 goat anti-mouse 488 diluted in PBST, is added. Because these two antibodies are fluorescents, they need to be protected from the light as much as possible, so the well is covered in a tin foil covering while incubating for an hour. After an hour, the samples are washed five times with shaking for five minutes each. The last step of the staining process is placing the slices on slides, and then gluing on a cover.

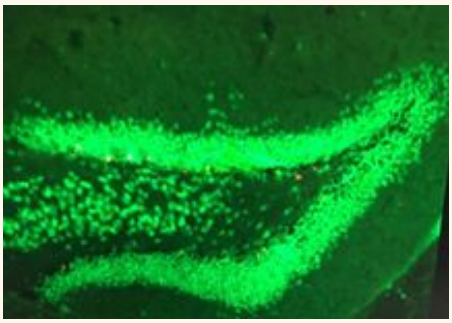

Figure 2. The green coloring is NeuN, and the red coloring is the BrdU.

To check the results of the injections and staining, the slides are put into an MBF Stereology microscope and pictures are taken via the SRS imaging system. When looking at the coloring on the microscope, BrdU brings out red coloring, indicating new cells, and NeuN brings out green coloring, indicating neurons. The best is when there are spots that are both red and green, indicating new neurons have formed and that the lactate was successful.

The Consistency of Motor and Perceptual Rhythmic Preferences and their Manifestations in Learning

Zachary Weiss
Advised under Dr. Elana Zion Golumbic and PhD student Anat Kliger

In a traditional environment when someone tries to learn by an auditory stimulus, such as through speech, there is what is known as a Preferred Rhythm (PR), a rhythm presented at a comfortable tempo. When a person is presented with a stimulus within this preferred range, it can be better learned through focusing than a stimulus at and beyond the extremes of the spectrum. An example of this is seen in classrooms when a teacher lectures in an excited tone and at a steady, nice pace, it is

easier for the students to commit the information to memory; in contrast, when a teacher presents information in a monotonous voice or rushes through material, a student learns less.

Findings[1] show there is a relationship between a person's Spontaneous Motor Tempo (SMT), and a person's performance in paced tasks. SMT is seen in lingering effects from paced tasks known as entrainment theory. As a participant is presented with auditory stimuli across a range of tempos, we can see a trend where the participants tap time interval becomes correlated with the actual stimulus interval time. This correlation is an indicator of a person's actual preferred tempo.

The experiment focuses on attention and finding a range of tempos at which the population can learn a presented auditory stimulus. The stimuli are presented as short rhythmical tones or prerecorded counting. The study had two parts: in the first, the participant listened to the stimulus, paused, and then continued tapping, while trying to match the stimulus. In the second part of the experiment, the participant was asked to synchronize with the stimulus in order to attempt to learn it better. The participant was then asked to continue tapping to match the presented stimulus rhythm. The tap time intervals of the participant were compared to the presented stimulus to show how well the stimulus was remembered.

The results showed that there was no significant difference between conditions of listen vs. sync, and tones vs. counting. These results allow us to switch over methods from synchronize and continuing with tones to listen and continuing with counting in the future EEG experiment. The results also show the training method has no significant difference in learning, but rather the difference is seen when the stimuli are presented within a person's PR range.

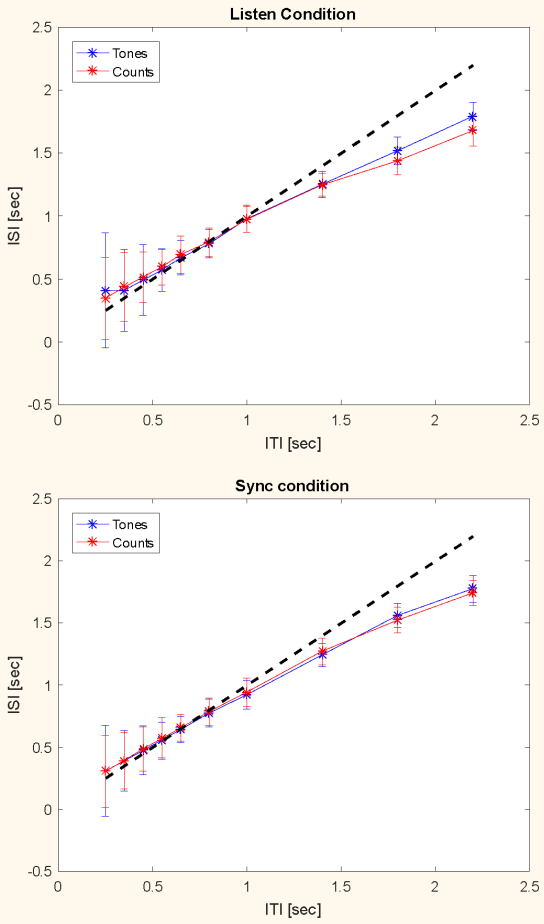

Figure 1 & 2. Comparison between the Tones and Counting Stimulus for the Listen and continue and Synchronize and continue conditions.

[1] *The Time of Our Lives: Life Span Development of Timing and Event Tracking* by Holub et al.